Molecular BioSystems

Accepted Manuscript

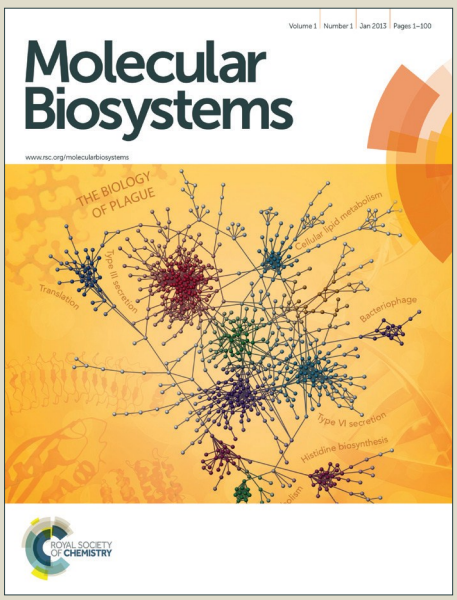

This is an *Accepted Manuscript*, which has been through the Royal Society of Chemistry peer review process and has been accepted for publication.

Accepted Manuscripts are published online shortly after acceptance, before technical editing, formatting and proof reading. Using this free service, authors can make their results available to the community, in citable form, before we publish the edited article. We will replace this *Accepted Manuscript* with the edited and formatted *Advance Article* as soon as it is available.

You can find more information about *Accepted Manuscripts* in the Information for Authors.

Please note that technical editing may introduce minor changes to the text and/or graphics, which may alter content. The journal's standard Terms & Conditions and the Ethical guidelines still apply. In no event shall the Royal Society of Chemistry be held responsible for any errors or omissions in this *Accepted Manuscript* or any consequences arising from the use of any information it contains.

ROYAL SOCIETY OF CHEMISTRY

www.rsc.org/molecularbiosystems

pH effect on the structural dynamics of cutinase from *Trichoderma reesei:* insights from molecular dynamics simulations

Mei Lin Duan[a], Lin Liu[a], Juan Du[a]*, Xiao Jun Yao[b]

[a] Key Lab of Applied Mycology, College of Life Science, Qingdao Agricultural University, Qingdao 266109, China

[b] College of Chemistry and Chemical Engineering, Lanzhou University, Lanzhou 730000, China

CORRESPONDING AUTHOR FOOTNOTE

* To whom correspondence should be addressed.

Email: dujuannx@126.com

Notes

The authors declare no competing financial interest.

Molecular BioSystems Accepted Manuscript

Abstract

Cutinases are utilized in a variety of industries for the hydrolysis of a broad range of substrates, such as cutin, polyesters, soluble esters, insoluble short- and long-chain triglycerides. The novel cutinase from *Trichoderma reesei* (*Tr*) attracted much attention for its two rare characteristics distinct from the classical cutinases: it possesses a lid covering its active site and its optimal activity at acidic pH. However, the structural basis on pH preference and the function of lid is still not well understood. In this work, total of six initial systems were set up either at acidic or basic pH conditions (closed-*apo*, open-*apo* and open-*holo*). Then, molecular dynamics (MD) simulations were performed to make a better understanding of structural dynamics of *Tr* cutinase under different pH conditions for the first time. The results mainly suggest that it is easier to open for the lid at an acidic pH condition. In addition, the binding of long-chain triglyceride is more stable at lower pH than higher pH. These findings elucidate that how pH influences *Tr* cutinase at atomistic level. The structural and dynamic details would be useful for rational enzyme design for acidic cutinase.

Introduction

Cutinase can hydrolyze a variety of substrates, such as cutin, polyesters, soluble esters, insoluble short- and long-chain triglycerides. The wide application in products and industrial processes of cutinases, including detergent and laundry industry, the textile industry, the food industry and the oil and fat industry and so on, has particularly made them attractive to intense research.[1-4] Cutinases share the same core of the α/β-hydrolase family, belonging to serine esterase.[5] The α/β-hydrolase fold contains eight β-sheets with several α-helices on either side.[6] They have a classical catalytic triad consisting of Ser, His and Asp, in which catalytic serine is not covered by an amphiphilic lid structure,[2] this often be believed to be responsible for the absence of interfacial activation. Lid converts from a closed to an open conformation at the present of the water-oil interface in most of lipases, producing large hydrophobic surfaces with relative portions of the active cavity, thus displaying strong affinity and sharply increased activity towards lipids.[7-9]

Molecular BioSystems Accepted Manuscript

Recently, a novel cutinase from *Trichoderma reesei* (*Tr* cutinase) has been found and its native and inhibitor-bound X-ray crystal structures have been obtained[10]. Interestingly, its two uncommon features also attracted our attention as mentioned above: one is it possesses a lid covering the active site in its closed conformation, similar to lipases. The other one is its optimum catalytic activity towards triglycerides at acidic pH condition.[10] *Tr* cutinase was defined as a new member of lipolytic enzymes exhibiting structural and kinetic properties of true lipases. Its optimum activity on short- and long-chain triglycerides was tested at pH 6, and it was inactive to short-chain triglyceride at pH 8, while the typical cutinase from *Fusarium solani* (*Fs*) displays optimum activity at pH 8 using the same pH-stat device.[10] Most reported cutinases show either non-existent or low activity at acidic pH. Nonetheless, it has been reported that other cutinases being active to cutin at below pH 4 recent years.[11-13] In industrial processing of acidic and alkaline environments, such as the process of acidic plant materials,[14] the findings of acidic cutinases can promote efficient hydrolysis as biocatalysts and improve its industrial application.[15] Therefore, the structural details of *Tr* cutinase at atomistic level will be helpful for the modification of enzyme.

In *Tr* cutinase, the lid is composed of helix α1 (Ser33-Lys43), helix α2 (Thr50-Gly70) and a hinge loop between them at the N-terminus (Fig. 1). Conformational rearrangements of the N-terminus (greater movement of helix α1 and slight rotation of helix α2) result in opening of the active cavity. Due to the lid completely covers the catalytic Ser164, activity would be possibly occur only when lid is open. In terms of lipases, many studies have been conducted over the years, especially by computational methods. For example, stuyding in the conformational changes,[16, 17] the mechanism of opening and closing of the lid,[18] the structural elements linked to the interfacial activity and the roles of the lid region in different solvent environments.[19-21] These studies show diversity of conformational changes of the lid region in lipases from different sources. It is certain that there are great differences between the lid of *Tr* cutinase and lipases (PDB ID: 1QGE[22] and 3O0D[16]) through comparing crystal structures (Fig. S1). Considering the importance of the lid region, whose mobility and behavior control the

Molecular BioSystems Accepted Manuscript

access of substrates to the active site of enzyme. So in our work, we attempt to make a more detailed understanding of the relationship between structure and function, and more importantly, try to explain how mobility of lid region affects catalytic activity.

In the same way, human gastric lipases (HGL) and dog gastric lipases (DGL) with lid are active under highly acidic surroundings.[23, 24] *Tr* cutinase may share some similarity with them. Experimental results indicated that gastric lipase prefers to bind to the oil-water interface at acidic pH condition.[25] Besides, Selvan et al[26] have conducted MD simulation to understand acid stability and domain movements of gastric lipases at an acidic pH and neutral conditions. They found the region with greatest fluctuations in the lid during MD simulation. This region has been considered to important for catalysis. The available information on lipases could shed light on our investigation.

In this work, based on the closed and open structures of *Tr* cutinase with and without a substrate, we performed MD simulation to make it possible to explore what aspects of protein structure, opening and mobility of the lid and substrates binding, are affected by different pH conditions, and how these aspects link to catalytic properties. It is indicated that pH affects the motion of the lid. Besides, the binding of long-chain triglyceride to active cavity at acidic pH can stabilize the global conformation of the enzyme-substrate complex. This study provides novel insight in understanding how pH influences *Tr* cutinase at atomistic level. The structural and dynamic details will be benefit for protein engineering for acidic cutinase.[27, 28]

Materials and Methods

Structure preparation and molecular docking

The crystal structures of *Tr* cutinase in closed (PDB ID: 4PSD) and open (PDB ID: 4PSE) conformation were used as initial coordinates. The major ingredient of olive oil called 1, 2, 3-trioleoylglycerol was used as the substrate molecule in this work. The structure of 1, 2, 3-trioleoylglycerol was sketched by Accelrys Discovery Studio 2.5 [29] and energy minimization was performed at the HF/6-31G* level of Gaussian09 program.[30] The topology and parameters for the 1, 2, 3-trioleoylglycerol was generated

Molecular BioSystems Accepted Manuscript

by the SwissParam server.[31] The protonation states of ionizable residues at pH 6 and 8 were determined based on the pK_a values predicted by H++ server,[32] respectively. To construct a model for *Tr* cutinase with substrate bound, AutoDock Vina program[33] was used to dock a 1, 2, 3-trioleoylglycerol into its open conformation structure. The complex with the lowest binding free energy was selected as the initial structure for simulation. All MD simulation systems were prepared with VMD 1.9.2,[34] including generation of the topology and coordinate files for the *Tr* cutinase in closed and open form at two pH conditions. Finally, there were six systems built for MD simulations study (Table. 1). The structures were visualized using PyMOL.[35]

MD simulation

MD simulations were conducted for each system of *Tr* cutinase using NAMD package 2.9[36] with CHARMM27 force field[37] for the protein. For explicit water simulations, TIP3P model[38] waters were used to solvate the systems in a periodic boundary cubic box extending up to 15 Å from the protein to boundary in each direction. The net charge of the protein before adding counter-ions is -6e and -10e at acidic and basic pH, respectivily. Sodium and chloride ions were added to make up a neutral solution of 0.15 M NaCl. For each system, energy minimization for 50000 time steps was carried out with a harmonic force constraint of 20 $kcal \cdot mol^{-1} \cdot Å^{-2}$ on the substrate and protein, substrate and backbone atoms of protein and substrate and alpha carbon atoms of protein, respectively. Then the temperature was gradually increased from 0 to 300 K within 200 ps under the *NVT* ensemble. The systems were relaxed within 2 ns from 20 to 0 kcal mol^{-1} $Å^{-2}$ under *NPT* ensemble condition. 38 ns MD production was performed for each system, except that the simulation was extended to 48 ns for the *apo*-open systems. For MD production, the temperature and pressure were kept constant using a Langevin thermostat and a Langevin barostat,[39] respectivily. The covalent bonds to hydrogen atoms were constrained using SHAKE algorithm[40] and the long electrostatic interactions was calculated by Particle Mesh Ewald (PME) method.[41] The cut-off for van der waals interactions was set to 12 Å. The time step was set to 2 fs. The atom coordinates were saved every 10 ps for trajectory analysis with VMD

Molecular BioSystems Accepted Manuscript

package. The time evolution data was smoothed by in-house script with an averaging interval of 100.

Results and discussion

pH influence the motion of the lid in closed state

In order to explore the structure and dynamics of this enzyme in the closed form at different pH conditions, MD simulations at pH 6 and pH 8 were performed. The structural stability of two systems was monitored by plotting the root-mean squared deviation (RMSD) of the backbone atoms. Fig. S2A shows that two systems stabilize after 25 ns and the RMSDs of protein are converged to 1.5 Å and 2.0 Å at pH 6 and pH 8, respectively. In addition, radius of gyrations (Rgs) (Fig. S2B) maintain stable during 20-40 ns, indicating the closed systems are well equilibrated. It is observed that some differences exist at two pH conditions. The values of RMSD and Rg are higher at pH 6 than pH 8. This implies pH have an influence on conformational changes of *Tr* cutinase in closed form.

Residues fluctuation in *Tr* cutinase during MD simulation in closed state is depicted in Fig. 2. The root-mean-square fluctuation (RMSF) of helix α1 (Ser33-Lys43) shows definite smaller conformational changes at pH 8 than the system at pH 6. Just as representative conformations extracted from MD trajectories in Fig. 2, helix α1 (main part of covering the active site) exhibits greater flexibility and sensitive response to the acidic pH condition. To some extent, it is indicated that the lid may open more easily in the environment of acidic pH condition, because the process of lid opening must be accompanied by greater lid displacements. Lipases are known to remain in a closed form in an aqueous environment.[16, 26] *Tr* cutinase with a lid structure controlling the access to active site may be keep it in the same way. As shown in Fig. S2, lid region maintained closed state in our simulation time scale for the closed structure in water.

Besides, by comparing the crystal structure of *Tr* cutinase in closed and open form, it is observed that some tight interactions between lid and core structure must be destroyed in the transition from closed to open state (Figures 1 and 3B), which mainly are the

Molecular BioSystems Accepted Manuscript

hydrogen bond interactions between Ile51 and Asp223, and Asp49 and Ile225. So the distances between them were calculated and plotted in Fig. 3A. It can be observed that both of the distances always are at H-bonding distance during MD simulation at pH 6 and pH 8 conditions. This is mostly consistent with the crystal structure. It implies that there are other important factors would destroy the strong interactions, such as the binding of the enzyme to a hydrophobic interface or the binding of substrate just like in the lipases.[16] Even so, some differences have also shown at two pH conditions, the distances are smaller at pH 8 than the system at pH 6. Rg profiles mentioned above for closed state at different pH conditions indicate a more compact structure at pH 8. In summary, we can conclude that the opening of the lid can't be observed in aqueous environment under the time scale simulated in this study. pH condition is one of the factors in regulating the opening process of the lid in *Tr* cutinase. More concretely, lid is more favorable to open at the acidic pH condition. As for the structural or environmental factors triggered the lid opening, the mechanism of this process would be explored in the further study.

The influence of pH condition on conformational stability of enzyme-substrate complex

Flexibility of the *Tr* cutinase structure

The structure of *Fs* cutinase co-crystallized with a short-chain triglyceride analogue (as an inhibitor) has been first studied by Longhi et al.[42] To our knowledge, there is no reported substrate co-crystallized structure of cutinases and little information is available about the structural dynamics of enzyme-substrate complex until now. For novel *Tr* cutinase with significant features, in order to understand the relationship between structure and pH-dependent catalytic activity, the current work is conducted. The results provide insights into global and local conformational changes through analyzing MD simulation trajectories.

RMSD and Rg of backbone atoms (Fig. S3) were calculated to check the stability of the open systems. It can be seen from Fig. S3 that *apo* and *holo* systems reach equilibrium after 5 ns and 20 ns, respectively. Rgs maintain stable during 20-40 ns,

Molecular BioSystems Accepted Manuscript

demonstrating a good convergence for open systems.

The RMSFs of the trajectories of open conformation relative to the native structure were calculated. It can be seen from Fig. 4A that there is little difference in *apo* state between pH 6 and pH 8. While the *holo* state (Fig. 4B) at pH 8 is more flexible than the system at pH 6 with an average value of 1.81 Å and 1.18 Å, respectively. The main flexible regions were identified in all of systems, which are the lid region (Asp30-Gly70) and region Cys212-Tyr232. The location of them in protein structure is shown in Fig. 5A. The latter is corresponding to the loop Cys171-Tyr191 in *Fs* cutinase, which is one of the substrate binding sites. The other two substrate binding sites are the region Arg88-Gly101 and Val122-Asn138 in *Tr* cutinase (Fig. 1) corresponding to Arg40-Gly52 and Val73-Ser91 respectively in *Fs* cutinase.[3] In early reviews about *Fs* cutinase, there were some statements that a "breath-like" movement in the mini-flap appears to exist in cutinase, which could be relative to substrate specificity.[43, 44] The movement involves the size of entrance of the active site, which is consisted of a small flap (residues Leu81-Ala85) and a binding loop (residues Cys178-Ala186) (Fig. S4).[8] In present systems, flexible helix α2 located above the latter two binding sites and region Cys212-Leu232 partially hinder the entrance of cavity, which is corresponding to this movement. They exhibit difference at two pH conditions as described latter.

Mobility of the lid region

Considering the lid structure is unique to *Tr* cutinase among classical cutinases of the same family. It covers the active site like true lipases, but the secondary structure elements and the position of the lid are different with the lipases. The role of this region in lipase is studied by Secundo et al,[45] it is proposed that the mobile lid plays an important role in regulating enzyme activity and substrate specificity *etc*. Therefore, it is necessary to focus on the mobility of the lid region in open form in aqueous solvent at different pH conditions. The *apo* state is used as a control, the lid in the *holo* state exhibits smaller conformational changes at acidic pH with lower RMSD values (Fig. 6B), while it undergoes great conformational changes at a basic pH. The great conformational changes are mainly attributed to the flexibility of helix α1 in the lid

Molecular BioSystems Accepted Manuscript

(Fig. 4B). In order to get easy observation of the lid mobility during MD simulation at the different pH conditions, the snapshots from each trajectory in open systems were extracted and displayed (Fig. 5). It is indicated that the helix α1 has the trend of being away from the core in some trajectories. The distance of Cα atom between residue Asn35 (in helix α1) and Asp223 (in the core region) was calculated and depicted in Fig. 7A and B, which can reflect the motion of the helix α1. As shown in Fig. 7A and B, the distance in the *holo* systems at pH 6 almost remains at 8 Å, it is close to the crystal structure, while it increases markedly, exceeding to 12 Å at pH 8. The H-bond between Asn35 and Asp223 H-bond exists in crystal structure of *Tr* cutinase. It is therefore possible to infer that it is a vital element to stabilize the helix α1. As expected, this H-bond takes about 90% occupation during the last 20 ns of simulation time at pH 6, while takes near zero at pH 8.

***Tr* cutinase prefers to bind the substrate at an acidic pH condition**

Comparing the RMSD and Rg (Fig. S3) of simulations of the four systems respectively, both of the RMSD and Rg have lower values at pH 6 than the case of pH 8 in the *holo* and *apo* systems, especially the average of RMSD is near 1.0 Å in the *Tr* cutinase with substrate-bound at pH 6, which is the pH condition with optimum activity.

Helix α1 and α2 together with region Cys212-Leu232 are responsible for the integrity of the active cavity. We previously mentioned that there is a clear trend of narrowing down of entrance of the active cavity. A detailed description of this finding is worth investigating further because size of the entrance is a key element for function of enzyme in general.[46] How the relative motion between the helix α2 and region Cys212-Leu232 represented the core over the equilibrium trajectories at different pH conditions changes? To elucidate this, the time evolution of distance is plotted in Fig. 7C and D. The distance between residue Ala54 and Ile224 can reflect the opening level of the active pocket entrance as displayed in Fig. 7E. In both of the *apo* and *holo* systems at pH 8, the relative distances are smaller than those at pH 6, especially the difference is apparent in the *holo* state. It means that helix α2 and region Cys212-Leu232 occur close to each other at pH 8, resulting in a more narrow active

Molecular BioSystems Accepted Manuscript

pocket entrance than the systems at pH 6. Besides, the other finding that helix α1 would be away from the core as mentioned previously is also worthy of our attention. The solvent accessible surface area (SASA) of active cavity was calculated for the common residues within 5 Å from substrate of the initial equilibrium structure in *holo* state at the two pH conditions, using VMD and a standard probe radius of 1.4 Å. In Fig. 8, the active cavity in *holo* system at pH 8 has an obvious larger SASA than that at pH 6, the majority of which is more than 3600 $Å^2$ with higher relative frequency. This cause disruption of integrity of the cavity and greater exposure to solvent for the active site at pH 8, which are not benefit to keep the substrate bound to the pocket. In summary, smaller conformational changes occur at pH 6 upon long-chain triglyceride bound to the cavity. It suggests that *Tr* cutinase prefers to bind the substrate at the acidic pH condition. This may explain that a heightened catalytic activity for long-chain triglycerides.

Conclusion

In the present study, the analysis of closed systems in *Tr* cutinase suggests the motion of the lid is affected by the surrounding pH conditions, especially the lower pH is the condition that lid tends to open easily. We constructed enzyme-substrate complex structure of *Tr* cutinase, through comparative analysis of two open-*holo* systems, conformational stability of enzyme-substrate complex is also influenced by pH. At acidic pH, the *holo* system undergoes smaller conformational changes, indicating that *Tr* cutinase prefers to bind substrates at acidic pH condition. The results obtained in MD simulations can explain that the optimal activity exhibited in *Tr* cutinase at acidic pH towards triglycerides. The key interactions that maintain the closed form were identified, such as hydrogen bond interactions between Ile51 and Asp223, and Asp49 and Ile225. In addtion, the relative motion between the helix α2 and region Cys212-Leu232 were proposed to reflect the opening level of the active pocket entrance, which would be key structural element for the enzyme activity. This study provided novel insight to understand the relationship between structure and function under different pH conditions of cutinase, which would be useful for rational enzyme

Molecular BioSystems Accepted Manuscript

design for acidic cutinase.

Conflict of interests

Authors declare no potential conflict of interest

Acknowledgements

This work was supported by the National Natural Science Foundation of China (Grant No. 31300599), the Talents of High Level Scientific Research Foundation (Grant No. 6631113318, 6631113326), the Graduate Research Plan "The study of relationship between structure and function of a novel cutinase and rational design" and Initial Foundation for Doctors (Grant No. 6631112308) of Qingdao Agricultural University.

Supporting Information

Fig. S1 Structure comparison of crystal structures of *Tr* cutinase and two lipases in closed form. The lid of *Tr* cutinase (PDB ID: 4PSD) and lipases (PDB ID: 1QGE and 3O0D) are colored red, cyan and purpleblue, respectivily.

Fig. S2 RMSD and Rg plots of backbone atoms of protein for closed form. (A) RMSD plots at pH 6 (blue line) and pH8 (red line); (B) Rg plots at pH 6 (blue line) and pH8 (red line).

Fig. S3 RMSD plots of backbone atoms of protein and Rg plots of backbone atoms of core protein with the exception of the lid for open form. RMSD plots for *apo* state (A) and *holo* state (B), at pH 6 (blue line) and pH8 (red line); Rg plots for *apo* state (C) and *holo* state (D), at pH 6 (blue line) and pH 8 (red line), respectively.

Fig. S4 Structure comparison of crystal structures of *Tr* and *Fs* cutinases in dark and light grey, respectively. The catalytic Ser164 is shown in stick representation. Region Cys212-Tyr232 and helix α2 in *Tr* cutinase are colored hotpink and magenta. Region Cys178-Ala186 and Leu81-Ala85 in *Fs* cutinase are colored greencyan and green, respectively.

Molecular BioSystems Accepted Manuscript

References

1. T. F. Pio and G. A. Macedo, *Advances in applied microbiology*, 2009, **66**, 77-95.
2. S. Chen, L. Su, J. Chen and J. Wu, *Biotechnology advances*, 2013, **31**, 1754-1767.
3. J. Li, L. Liu, S. Chen, G. Du and J. Chen, *Chinese journal of biotechnology*, 2009, **25**, 1829-1837.
4. D. Ribitsch, E. Herrero Acero, A. Przylucka, S. Zitzenbacher, A. Marold, C. Gamerith, R. Tscheliessnig, A. Jungbauer, H. Rennhofer, H. Lichtenegger, H. Amenitsch, K. Bonazza, C. P. Kubicek, I. S. Druzhinina and G. M. Guebitz, *Applied and environmental microbiology*, 2015, **81**, 3586-3592.
5. C. M. L. Carvalho, M. R. Aires-Barros and J. M. S. Cabral, *Electronic journal of biotechnology*, 1998, **1**, 1-14.
6. H. Jochens, M. Hesseler, K. Stiba, S. K. Padhi, R. J. Kazlauskas and U. T. Bornscheuer, *Chembiochem : a European journal of chemical biology*, 2011, **12**, 1508-1517.
7. S. Longhi and C. Cambillau, *Biochimica et biophysica acta*, 1999, 185-196.
8. M. R. Egmond and J. d. Vlieg, *Biochimie*, 2000, **82**, 1015-1021.
9. C. Martinez, A. Nicolas, H. v. Tilbeurgh, M.-P. Egloff, C. Cudrey, R. Verger and C. Cambillau, *Biochemistry*, 1994, **33**, 83-89.
10. A. Roussel, S. Amara, E. Mateos-Diaz, S. Blangy, H. Kontkanen, A. Westerholm-Parvinen, F. Carrière and C. Cambillau, *Journal of molecular biology*, 2014, **426**, 3757–3772.
11. N. Antti, P. Ville, H. Mari, K. Hanna, S. Markku and N. S. Tiina, *Applied microbiology and biotechnology*, 2014, **98**, 3639-3650.
12. H. Xu, Q. Yan, X. Duan, S. Yang and Z. Jiang, *Food chemistry*, 2015, **188**, 439-445.
13. A. Nyyssola, V. Pihlajaniemi, R. Jarvinen, S. Mikander, H. Kontkanen, K. Kruus, H. Kallio and J. Buchert, *Enzyme and microbial technology*, 2013, **52**,

Molecular BioSystems Accepted Manuscript

272-278.

14. H. Daniell, US 20090325240 A1, 2009-12-31.
15. A. Nyyssölä, *Applied microbiology and biotechnology*, 2015, **99**, 4931-4942.
16. F. Bordes, S. Barbe, P. Escalier, L. Mourey, I. Andre, A. Marty and a. S. Tranier, *Biophysical journal*, 2010, **99**, 2225-2234.
17. S. Barbe, J. Cortes, T. Simeon, P. Monsan, M. Remaud-Simeon and I. Andre, *Proteins*, 2011, **79**, 2517-2529.
18. Y. Jiang, L. Li, H. Zhang, W. Feng and T. Tan, *Journal of chemical information and modeling*, 2014, **54**, 2033-2041.
19. M. A. Brzozowski, H. Savage, C. S. Verma, J. P. Turkenburg, D. M. Lawson, A. Svendsen and S. Patkar, *Biochemistry*, 2000, **39**, 15071-15082.
20. M. Cheng, C. Angkawidjaja, Y. Koga and S. Kanaya, *The FEBS journal*, 2012, **279**, 3727-3737.
21. M. Z. A. Rahman, A. B. Salleh, R. N. Z. R. A. Rahman, M. B. A. Rahman, M. Basri and T. C. Leow, *Protein science : a publication of the Protein Society*, 2012, **21**, 1210-1221.
22. S. Barbe, V. Lafaquière, D. Guieysse, P. Monsan, M. Remaud-Siméon and I. André, *Proteins: Structure, Function, and Bioinformatics*, 2009, **77**, 509-523.
23. A. Roussel, N. Miled, L. Berti-Dupuis, M. Riviere, S. Spinelli, P. Berna, V. Gruber, R. Verger and C. Cambillau, *The Journal of biological chemistry*, 2002, **277**, 2266-2274.
24. A. Roussel, S. Canaan, M. P. Egloff, M. Riviere, L. Dupuis, R. Verger and C. Cambillau, *The Journal of biological chemistry*, 1999, **274**, 16995-17002.
25. H. Chahinian, T. Snabe, C. Attias, P. Fojan, S. B. Petersen and F. C. re, *Biochemistry*, 2006, **45**, 993-1001.
26. A. Selvan, C. Seniya, S. N. Chandrasekaran, N. Siddharth, S. Anishetty and G. Pennathur, *FEBS letters*, 2010, **584**, 4599-4605.
27. C. Roth, R. Wei, T. Oeser, J. Then, C. Follner, W. Zimmermann and N. Strater, *Applied microbiology and biotechnology*, 2014, **98**, 7815-7823.
28. Z. Liu, Y. Gosser, P. J. Baker, Y. Ravee, Z. Lu, G. Alemu, H. Li, G. L.

Molecular BioSystems Accepted Manuscript

Butterfoss, X. P. Kong, R. Gross and J. K. Montclare, *Journal of the American chemical society*, 2009, **131**, 15711-15716.

29. *Discovery Studio,version 2.5.5; Accelrys Software, Inc. San Diego, CA*, 2010.
30. M. J. Frisch, G. W. Trucks, H. B. Schlegel, G. E. Scuseria, M. A. Robb, J. R. Cheeseman, G. Scalmani, V. Barone, B. Mennucci, G. A. Petersson, H. Nakatsuji, M. Caricato, X. Li, H. P. Hratchian, A. F. Izmaylov, J. Bloino, G. Zheng, J. L. Sonnenberg, M. Hada, M. Ehara, K. Toyota, R. Fukuda, J. Hasegawa, M. Ishida, T. Nakajima, Y. Honda, O. Kitao, H. Nakai, T. Vreven, J. A. Montgomery Jr., J. E. Peralta, F. Ogliaro, M. J. Bearpark, J. Heyd, E. N. Brothers, K. N. Kudin, V. N. Staroverov, R. Kobayashi, J. Normand, K. Raghavachari, A. P. Rendell, J. C. Burant, S. S. Iyengar, J. Tomasi, N. R. M. Cossi, N. J. Millam, M. Klene, J. E. Knox, J. B. Cross, V. Bakken, C. Adamo, J. Jaramillo, R. Gomperts, R. E. Stratmann, O. Yazyev, A. J. Austin, R. Cammi, C. Pomelli, J. W. Ochterski, R. L. Martin, K. Morokuma, V. G. Zakrzewski, G. A. Voth, P. Salvador, J. J. Dannenberg, S. Dapprich, A. D. Daniels, Ö. Farkas, J. B. Foresman, J. V. Ortiz, J. Cioslowski and D. J. Fox, *Gaussian, Inc., Wallingford, CT, USA*, 2009.
31. V. Zoete, M. A. Cuendet, A. Grosdidier and O. Michielin, *Journal of computational chemistry*, 2011, **32**, 2359-2368.
32. J. C. Gordon, J. B. Myers, T. Folta, V. Shoja, L. S. Heath and A. Onufriev, *Nucleic acids research*, 2005, **33**, W368-371.
33. O. Trott and A. J. Olson, *Journal of computational chemistry*, 2010, **31**, 455-461.
34. W. Humphrey, A. Dalke and K. Schulten, *Journal of molecular graphics*, 1996, **14**, 33-38.
35. Schrödinger and LLC, *The PyMOL Molecular Graphics System, Version 1.3.1*, 2010.
36. J. C. Phillips, R. Braun, W. Wang, J. Gumbart, E. Tajkhorshid, E. Villa, C. Chipot, R. D. Skeel, L. Kalé and K. Schulten, *Journal of computational chemistry*, 2005, **26**, 1781-1802.

Molecular BioSystems Accepted Manuscript

37. A. D. Mackerell, Jr., M. Feig and C. L. Brooks, 3rd, *Journal of computational chemistry*, 2004, **25**, 1400-1415.

38. W. L. Jorgensen, J. Chandrasekhar, J. D. Madura, R. W. Impey and M. L. Klein, *The journal of chemical physics*, 1983, **79**, 926-935.

39. T. X. Xiang, F. Liu and D. M. Grant, *The journal of chemical physics*, 1991, **94**, 4463-4471.

40. T. G. Coleman, H. C. Mesick and R. L. Darby, *Annals of biomedical engineering* 1977, **5**, 322-328.

41. D. Tom, Y. Darrin and P. Lee, *The Journal of chemical physics*, 1993, **98**, 10089-10092.

42. S. Longhi, M. Mannesse, H. M. Verheij, G. H. De Haas, M. Egmond, E. Knoops-Mouthuy and C. Cambillau, *Protein science : a publication of the Protein Society*, 1997, **6**, 275-286.

43. E. P. Melo, S. l. M. B. Costa, J. M. S. Cabral, P. Fojan and S. B. Petersen, *Chemistry and physics of lipids*, 2003, **124**, 37-47.

44. C. M. Carvalho, M. R. Aires-Barros and J. M. Cabral, *Biotechnology and bioengineering*, 1999, **66**, 17-34.

45. F. Secundo, G. Carrea, C. Tarabiono, P. Gatti-Lafranconib, S. Broccab, M. Lotti, K.-E. Jaeger, M. Puls and T. Eggert, *Journal of molecular catalysis B: enzymatic*, 2006, **39**, 166-170.

46. A. Gora, J. Brezovsky and J. Damborsky, *Chemical reviews*, 2013, **113**, 5871-5923.

Molecular BioSystems Accepted Manuscript

Table 1. Summary of the six simulation systems

systems	starting structure	water molecules	total atoms	time
close-pH6	X-ray structure (PDB ID: 4PSD)	10622	35157	40 ns
close-pH8		10617	35142	40 ns
apo-pH6	X-ray structure (PDB ID: 4PSE)	12573	40973	50 ns
apo-pH8		12570	40964	50 ns
holo-pH6	Docked 1,2,3-trioleoylglycerol into 4PSE	13081	42668	40 ns
holo-pH8		13075	42650	40 ns

Molecular BioSystems Accepted Manuscript

Figure Captions

Fig. 1 Initial structures of *Tr* cutinase in MD simulation: closed and open conformation are presented by dark and light shading, respectively. Helix α1 and α2 connected by a loop (consist of lid) are colored red and blue; regions Cys212-Tyr232, Arg88-Gly101, and Val122-Asn138 are colored pink, cyan and purple, respectively. The active site is colored yellow.

Fig. 2 RMSF of heavy atoms of closed system at pH 6 (black) and pH 8 (red). Two representative snapshots of lid region extracted from trajectories at pH 6 (left) and pH 8 (right) are showed in cartoon models.

Fig. 3 (A) The relative distribution of two distances from the lid to the core in closed systems at pH 6 (solid lines) and pH 8 (dash-dotted lines). (B) Cartoon representation of the two distances in crystal structure.

Fig. 4 RMSFs of heavy atoms of open systems. (A) *apo* state at pH 6 (blue) and pH 8 (red); (B) *holo* state at pH 6 (blue) and pH 8 (red).

Fig. 5 Snapshots of *Tr* cutinase structures in open systems. The color is coded by the rmsf, with blue being the lowest fluctuations to white to red being the highest fluctuations. *apo* state at pH 6 (A) and pH 8 (B); *holo* state at pH 6 (C) and pH 8 (D).

Fig. 6 RMSDs of backbone atoms of lid region (residues 30-70) in open systems during MD simulation. (A) *apo* state at pH 6 (blue) and pH8 (red); (B) *holo* state at pH 6 (blue) and pH 8 (red).

Fig. 7 The relative distribution of distances in open systems. One reflects the trend of helix α1 being away from the core: (A) *apo* state at pH 6 (solid line), (B) *apo* state at pH 8 (dash-dotted line); the other one represents the opening level of entrance of the active cavity: (C) *apo* state at pH 6 (solid line), (D) *holo* state at pH 8 (dash-dotted line).

Fig. 8 The SASAs distribution of residues within 5 Å from substrate of the initial equilibrium structure. (A) and (B) *apo* and *holo* state at pH 6 (solid line) and pH 8

Molecular BioSystems Accepted Manuscript

(dash-dotted line), respectively.

Molecular BioSystems Accepted Manuscript

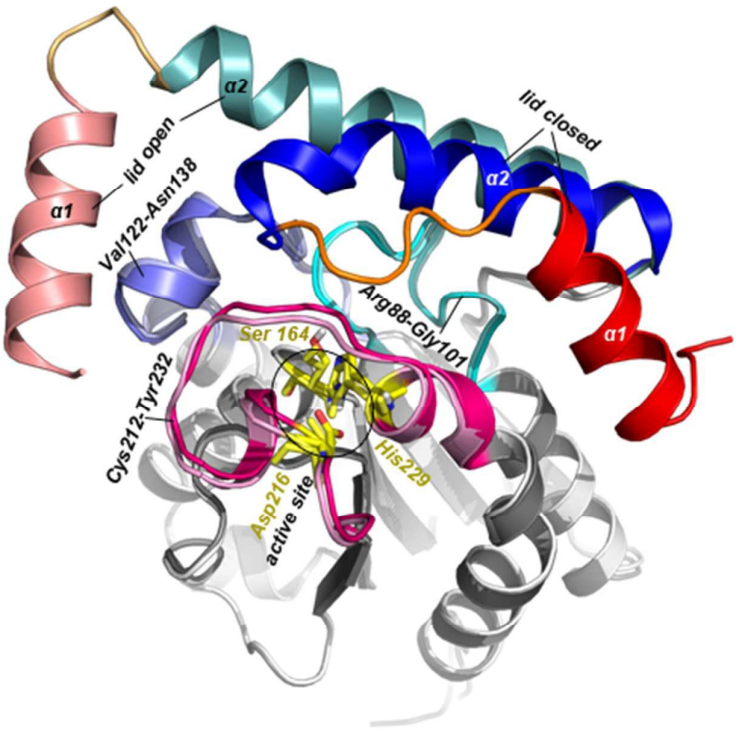

Fig. 1

Molecular BioSystems Accepted Manuscript

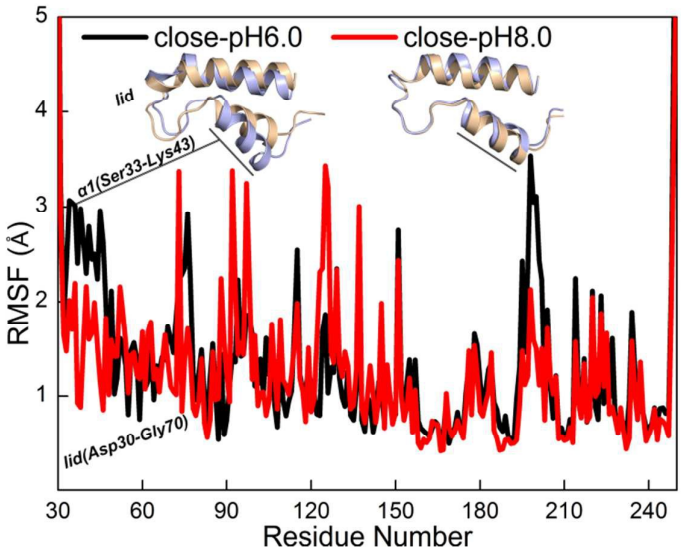

Fig. 2

Molecular BioSystems Accepted Manuscript

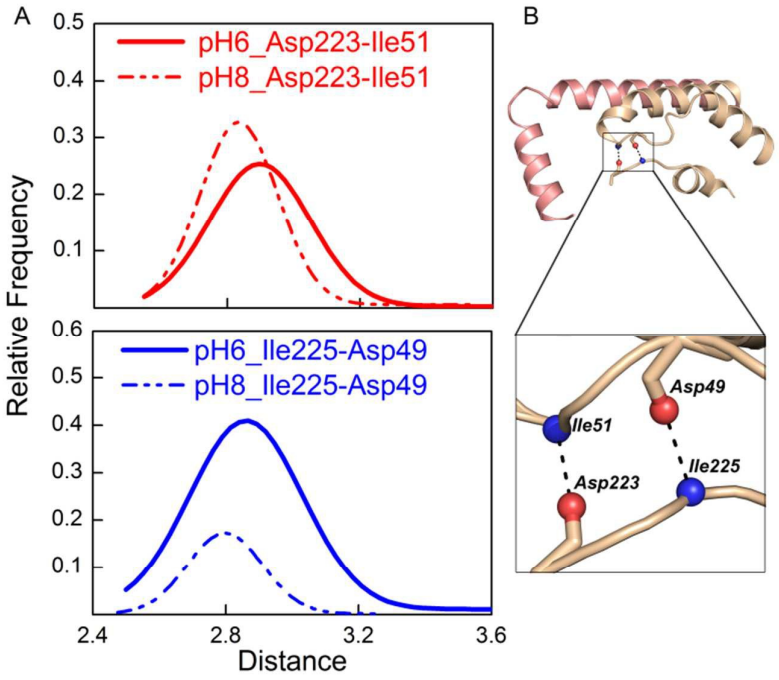

Fig. 3

Molecular BioSystems Accepted Manuscript

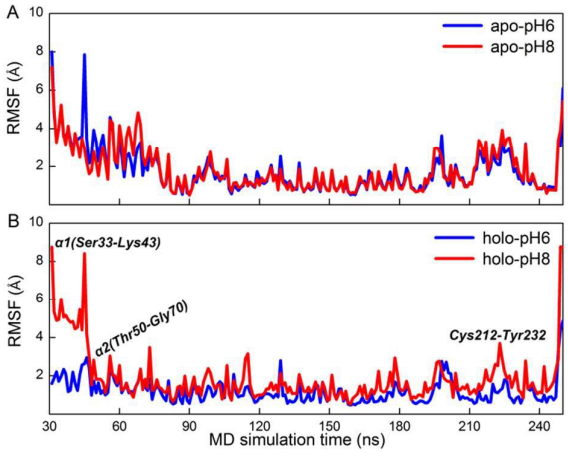

Fig. 4

Molecular BioSystems Accepted Manuscript

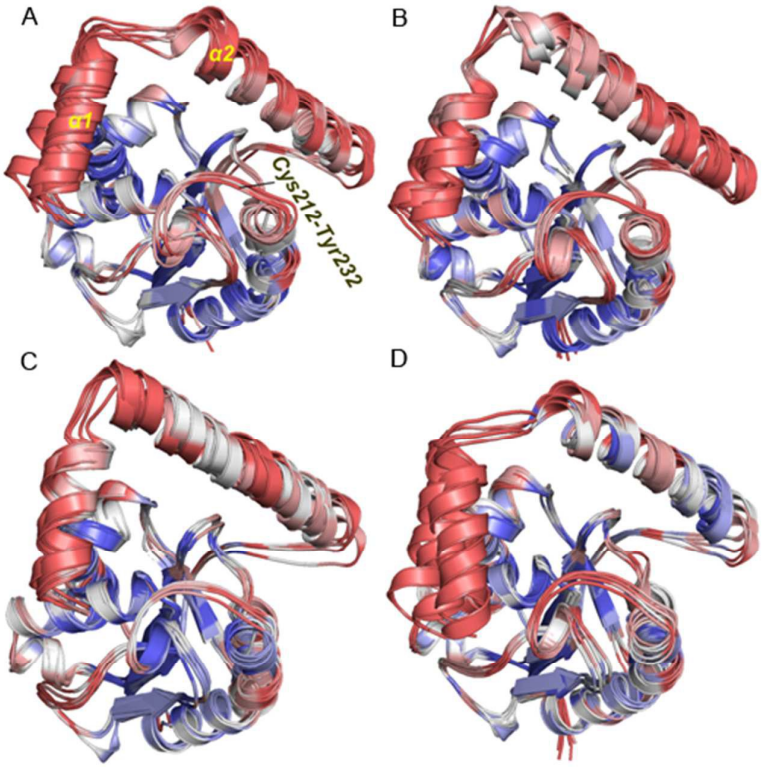

Fig.5

Molecular BioSystems Accepted Manuscript

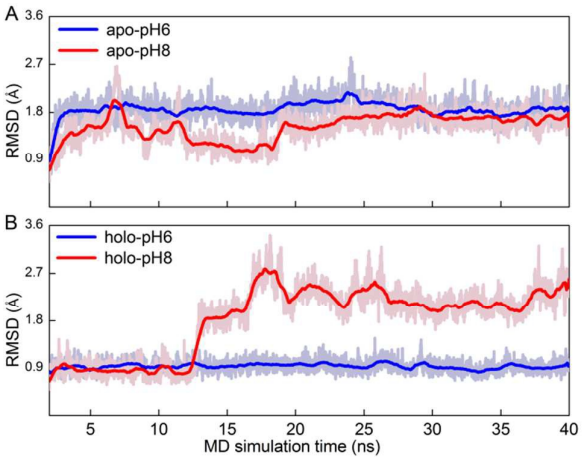

Fig. 6

Molecular BioSystems Accepted Manuscript

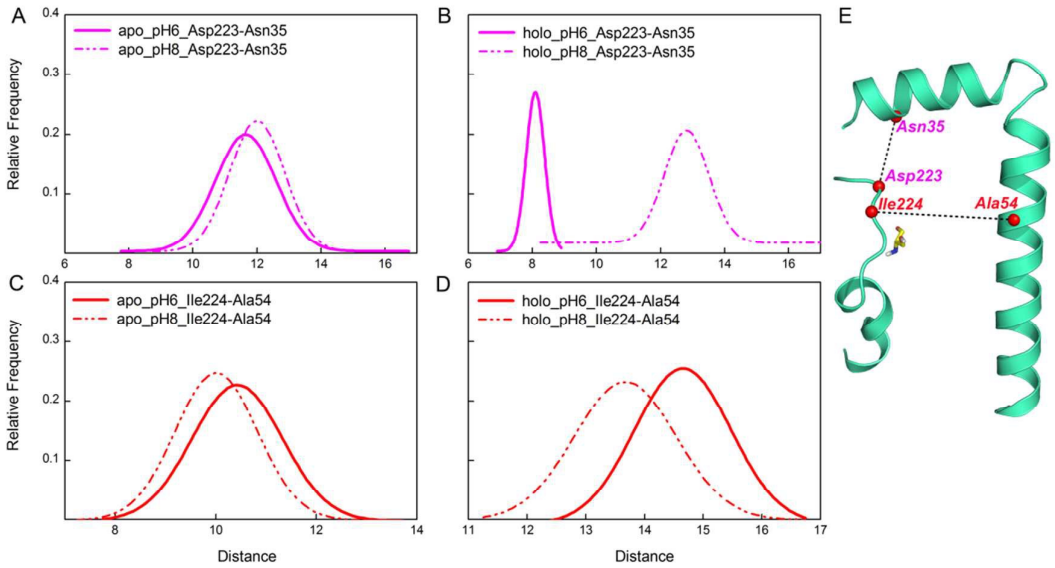

Fig. 7

Molecular BioSystems Accepted Manuscript

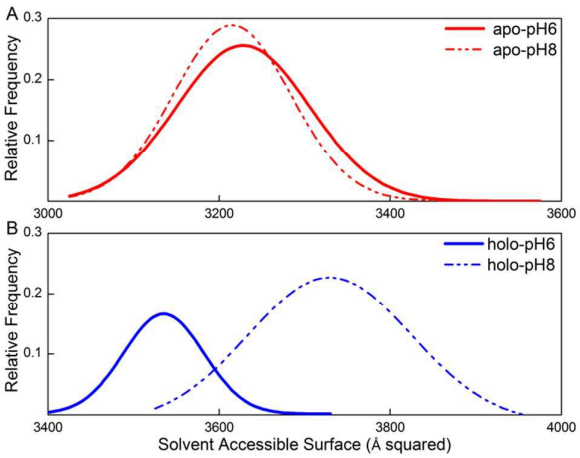

Fig .8

Molecular BioSystems Accepted Manuscript